THE DETERMINATION OF THE STRUCTURE AND COMPOSITION AT INTERFACES TO ATOMIC RESOLUTION

C.B. BOOTHROYD, C.S. BAXTER, E.G. BITHELL, M.J. HÿTCH, F.M. ROSS, K. SATO and W.M. STOBBS

Department of Materials Science and Metallurgy, University of Cambridge, Pembroke Street, Cambridge, CB2 3QZ, UK

The prediction of the properties of modern multilayered systems provides a challenge to the accuracy to which the structure of a boundary can be characterised using the transmission electron microscope (TEM). A variety of new ways of using the TEM have recently been developed in this context, and here we describe some of the approaches which are now being applied. Particular emphasis is given to a description of the strengths and weaknesses of the Fresnel method in its potentially broad application to compositional analysis.

1. Introduction

The properties of many materials depend upon the structural and compositional variations in the interfaces present so that such boundaries have to be characterised before the properties can be understood. This is as true for semiconductor materials such as GaAs/AlGaAs heterostructures – for which the precise structure and degree of misorientation of the GaAs/AlGaAs interfaces present can determine the optical properties of a device – as it is for metallic alloys, the hardness and strength of which can often depend on the nature and form of segregants at the grain boundaries. The better the boundaries can be characterised, the better the practical understanding of the properties. For many years electron microscopy has been used mainly qualitatively so that only phenomenological comparisons of the irregularities of a microstructure could be discussed in relation to the behaviour of the material examined. The development of the weak beam technique [1] set the scene for a more quantitative approach, for example to the correlation of the mechanical properties with measured changes of stacking fault energy. Yet the apparent ease with which high resolution imaging allows an atomic structure to be visualised has inhibited the understanding of how misleading these images can sometimes be, and has also hindered the introduction of directly applicable and more readily quantifiable approaches to structural characterisation.

Here we will describe the work which has been done, in the main in our own laboratory, on the development of a range of new methods which we hope will, in the future, enable a structure to be characterised to sufficient accuracy to allow the measurements to be used in modelling of behaviour with a reduced number of free parameters.

We can divide the structural features requiring measurement into two classes, these being associated respectively with the nature and form of any compositional irregularity and with the characteristics of the local displacements at and around the interfaces. The first of these includes "large-scale" compositional changes which might occur from one side of a boundary to the other as well as the smaller-scale (< 1 nm) changes associated with the presence of segregation. The second set of structural properties of interest includes the magnitude of the rigid body displacement across the boundary (if it separates two grains of the same phase), the measurement of the strain associated with a boundary between two phases, and in both these cases the characterisation of any interfacial

defects. We will first discuss the transmission electron microscopical (TEM) techniques that can be used for the two overall types of characterisation needed and then give examples of the application of these techniques to some of the more interesting interface problems which we are investigating.

2. Quantitative TEM methods

2.1. Composition changes across the interface

The simplest property of an interface to measure is the composition change across it, at least at the low resolution provided by an energy-dispersive X-ray spectroscopy (EDXS) or electron energy loss spectroscopy (EELS) probe. However, when better resolutions than the available probe size are required, such as when measuring the composition of nanometre-scale layers of a GaAs/AlGaAs heterostructure, more indirect methods have to be used. One available approach takes advantage of the correlation of lattice parameter with composition: the relatively high accuracy with which lattice parameters can be measured using HOLZ patterns allows the composition of localised regions to be determined sufficiently accurately to be useful. The spatial resolution is again limited by, and is certainly no better than, the probe size. Other quantitative methods exploit the dependence of electron scattering on atomic number in order to enable compositions to be determined from intensities recorded in images. One approach has been demonstrated by Kakibayashi and Nagata [2,3]: a 90° wedge of AlGaAs is imaged along [100] allowing, in principle, the aluminium content to be deduced from the position of the bright field thickness fringes. The same method is expected to be applicable to other compound semiconductors, but the analysis will be complicated by strain effects originating from the interfaces between layers of different compositions. Furthermore, absorption has to be dealt with carefully [4] and worries remain about irregularities in the cleavage [5] so that other methods based on the same principle can be more useful. In fact, for many materials, such as alloys which undergo spinodal decomposi-

tion, the measurement of the intensity changes associated with carefully chosen dark field reflections allows accurate characterisation of the composition changes (e.g. ref. [6]). The principle of the dark field approach can be readily appreciated by considering the classic example of the AlGaAs structure for which the amplitude of the 002 reflection is sensitively dependent upon the Al/Ga ratio [7]. However, accurate results can be obtained only when the inelastic scattering behaviour is taken into account [8] and systems have been found for which the technique gives anomalous results [9]. The ultimate spatial resolution of composition determinations made using dark field images will typically be about 0.5 nm (though image digitisation problems can sometimes increase this figure) and is limited by the Airy spread function of the objective aperture.

The resolution of these imaging techniques, though remarkable when compared with that attainable by direct EDXS or even EELS methods, is nevertheless insufficient for many interesting interface problems. The highest possible resolution is required, for example, for the determination of the thickness of the SiO_x layer at a Si/SiO_2 interface or for the measurement of the abruptness of the interfaces in GaAs/AlGaAs heterostructures. In this latter example a local composition change at the monolayer level can change the electronic properties while in the former the structure of the intermediate layer is indicative of the oxidation mechanism.

It is thus fortunate that a localised composition change is associated with an equally localised change in the mean forward scattering potential. This in turn affects the form and intensity of the Fresnel fringe profiles seen in the TEM when a vertical boundary is imaged slightly out of focus. It has been demonstrated [10] that the intensity of the Fresnel fringes is to first order proportional to the magnitude of the change in the scattering potential and thus to the composition change, while the form of the fringes is more closely related to the abruptness of the composition change [11]. The nature of the element of interest (for example the segregant at an interface) still has to be determined by a method such as EELS, but the magnitude and form of the local concentration

changes can, in principle, be more accurately quantified from Fresnel data, and the more accurately so the more localised the composition changes (in the sub-2 nm range). In this sense the Fresnel technique is therefore complementary to EELS. The method is still being developed and care has to be taken in its use both when the scattering potential changes are very large [12] and when there is strong dynamical contrast [10,13].

2.2. Interface structure

There are three aspects of interface structure which have to be considered, these being: (1) the magnitude of any rigid body displacement of one grain with respect to the other, (2) the form of large scale strain fields caused by the mismatch of the lattices on either side of the interface, and (3) the characterisation of any local strain fields caused by intrinsic dislocations or interfacial steps on the boundary itself.

At first sight it might be thought to be easy to determine rigid body displacements directly from high resolution micrographs of "edge-on" interfaces, but in practice two problems prevent such a direct approach from being accurate. From a fundamental point of view, in order to measure the small (< 0.01 nm) shifts in atomic positions near the interface, information out to at least the second Fourier component of the lattice spacing is required, and for most materials this is far beyond the microscope resolution limit. The lattice fringes in the image will not in general yield a true representation of the local atomic positions near to the interface even when the specimen can be treated as a weak phase object. More seriously, the comparison of image series with simulations rarely provides a well-defined solution of an unknown structure because the relevant microscope and specimen parameters (defocus, C_s, beam tilt, specimen thickness, etc.) usually cannot be determined to sufficient accuracy. However, for the case where there is a common Bragg reflection across the interface and the imaging conditions are identical on both sides of it (this being a situation which can be realised, for example, for a $\Sigma 3$ twin boundary), any lattice fringe shifts due to the microscope conditions will be constant across the

interface. Any measured image shift, as determined from data for regions relatively distant from the interface, will accurately represent the rigid body displacement. This method has been used to determine displacements of less than about 0.004 nm for Au and Cu boundaries [14,15]. The fringe positions close to the interface will still be affected by the limited transfer of the microscope, but a "resolution" far better than that of the microscope itself can be obtained by averaging over sufficient lattice fringes, the accuracy of the method being limited only by the sizes of the regions which are scattering uniformly.

The large-scale periodic strains produced when the materials on either side of the interfaces in strained coherent multilayers have different lattice parameters (as can be achieved in the Cu/Ni-Pd, GaAs/InGaAs or Si/Si-Ge systems, amongst others) can also be measured, at least in principle, by the application of high resolution methods [16]. If the wavelength of the multilayer is large enough then the change in lattice spacing across the multilayer can be determined by comparing the actual position of each lattice fringe with the average lattice fringe pattern. For smaller multilayer wavelengths (of less than about twenty atomic layers) the lattice spacing cannot be measured to sufficient accuracy to allow the detection of strains which are typically less than about 5%, but useful structural information can often still be obtained by comparing the average lattice fringe spacing parallel and perpendicular to the layers [17]. Even though the atomic configurations are not required it is of course still necessary to compare the images obtained with simulations of multilayers including modelled elastic strains before the measured values can be interpreted. This in turn requires that both the layer compositions and the degree of interdiffusion across the layers are known. Fortunately the composition profile can be measured to sufficient accuracy using the Fresnel method, as outlined briefly above.

The difficulties involved in making structural characterisations of the large-scale displacements and strains sufficiently accurate to be useful are compounded when attempting to use HREM to characterise the local form of interface defects or steps. There are two separate aspects of the prob-

lem to be considered in the characterisation of such defects. Firstly it is necessary to be able to image the local variation in composition to a resolution of about one atomic spacing. Secondly, the positions of the atoms surrounding the defect must be measured to accuracies considerably better than this in order to deduce the defect strain field. Determining the effects of the change in composition in parallel with those caused by a local step is particularly difficult in epitaxial semiconductor heterostructures such as GaAs/AlGaAs for which there is no difference in crystal structure across the interface. For this system interfacial steps have only been detected with any confidence for the extreme composition difference between the two binaries [18,19]. In principle an enhancement of the contrast caused by the composition change across the interface can be obtained by using a central beam stop aperture in the HREM. This has the effect of increasing the relative contribution to the image from the more compositionally sensitive diffracted beams. However, it has been demonstrated that under centre stop imaging conditions the detail contributed by inelastically scattered electrons can still dominate the image thus obscuring the compositional contrast [20,21]. Any attempt to measure the strain field around an interfacial step by direct high resolution methods is limited, as it is for bulk displacements, by the need to transfer at least the second Fourier component of the lattice spacing in order for the image to faithfully represent the local lattice distortions. Clearly the popular approach of Fourier filtering the image obtained will, while it makes the detection of a boundary defect easier, equally reduce the accuracy to which the displacement field can be measured. It seems clear that weak beam techniques, even if also difficult to quantify, represent the only real hope for the measurement of weakly varying displacement fields [22,23].

3. Examples of interface characterisation

We give below various detailed examples of the applications of the techniques described above. These illustrate a variety of aspects of interfacial characterisation, and emphasise how the selection of a particular technique depends upon both the material under consideration and the information sought. The examples considered are:

(1) Si/SiO_2 interfaces: this is an example of the successful application of the Fresnel technique to the determination of compositions at a graded interface.

(2) Grain boundary segregation: here we expect the Fresnel method to have useful applications.

(3) Strained multilayers: these illustrate the essential combined application of Fresnel and high resolution techniques but also exemplify the additional problems inherent in characterising strained materials.

(4) GaAs/AlGaAs heterostructures: this is another example of the successful application of techniques for determining composition profiles. Also of interest for such systems is the characterisation of interfacial defects, and it is explained why this requires further development of high resolution techniques.

3.1. Si / SiO_2 interface

The first problem we consider is the characterisation of Si/SiO_2 interface using the Fresnel technique. The interest in this interface arises because, despite the considerable amount of work that has been done using a wide variety of techniques, questions remain to be answered on the thickness of the layer of any intermediate stoichiometry. It is the measurement of the form of such an intermediate layer which will allow currently competing models for the oxidation process to be tested. Accordingly, specimens have been examined which were oxidised under a wide range of conditions. Fig. 1 shows part of a through-focal series of images of thin silica together with the digitised fringe profiles obtained from them. The work is described in more detail elsewhere [11,24] but here we can note that the Fresnel fringe spacings and intensities (as defined in fig. 2) can be used to obtain the compositional change and its form. The thickness of the oxide layer is determined by plotting the separation of the first Fresnel fringes (d in fig. 2) against defocus, as shown in fig. 3. The composition of the
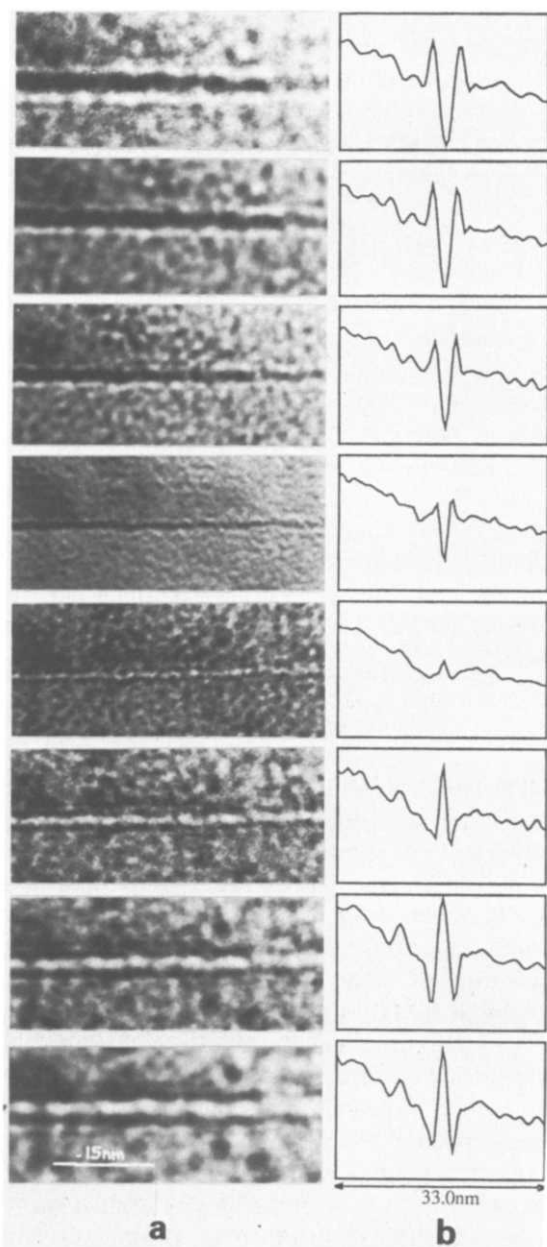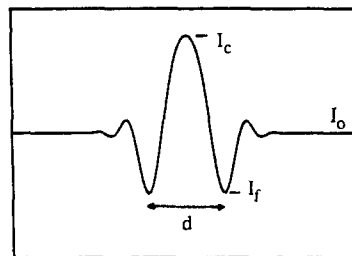
Fig. 2. Diagram defining the terms I_0, I_c, I_f and d as measured from the experimental Fresnel profiles.

oxide layer is the most important parameter in determining the intensity of the Fresnel fringes, i.e. the values of $(I_c - I_0)/I_0$ and $(I_f - I_0)/I_0$. These ratios are plotted as a function of specimen thickness in fig. 4 for a fixed defocus. Also shown in fig. 4 are the lines representing contrast values calculated from theory for an assumed stoichiometric oxide. It can be seen that although the theoretical contrast values fit the experimental values for the lowest specimen thicknesses examined, for higher thicknesses the measured contrast is always lower than the theory suggests. The most probable explanation for this lies in the way inelastic scattering can contribute, in differing degrees, to the Fresnel fringes and to the background. This is difficult to model, but the lines marked B in fig. 4 are the contrast values calculated when the effects of plasmon scattering are included in the simulations. As can be seen the inclusion of plasmon scattering improves the fit of the experimental values with the modelled contrast but we believe that it will also be necessary to include the complicated effects of, in particular,
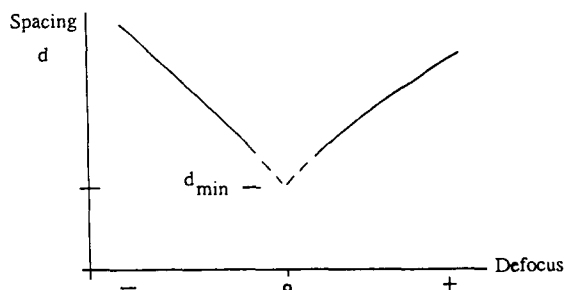

Fig. 1. (a) Part of a through focal series of images of a thin silicon oxide layer seen edge-on. The oxide layer was grown on single crystal silicon (lower half of each image) and was later capped with a layer of polycrystalline silicon (upper half). From bottom to top is under- to overfocus in steps of 430 nm. (b) Fresnel fringe profiles obtained from the micrographs in (a) by digitising and averaging small regions along the direction of the oxide layer. The intensity scale is arbitrary with low values representing dark regions of the positive print.

Fig. 3. Schematic diagram of the variation of fringe spacing d with defocus. Near zero defocus the data is uncertain because the fringe contrast is low (as in the central profile of fig. 1b).
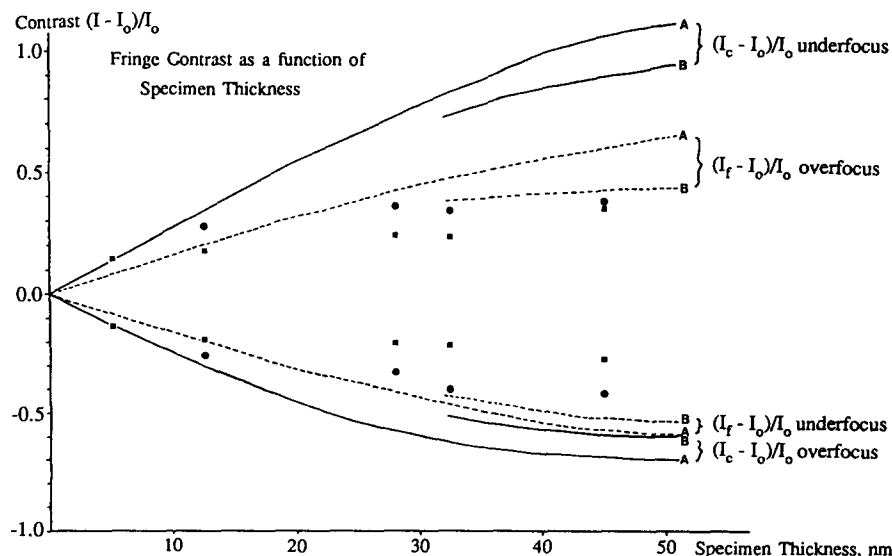
Fig. 4. The effect of inelastic scattering on Fresnel contrast. On this graph circles and squares show the values of $(I_c - I_0)/I_0$ and $(I_f - I_0)/I_0$ respectively for two particular values of defocus, $+430$ nm and -430 nm. Theoretical lines marked A are contrast values obtained from a non-atomistic multislice calculation at the correct defocus, oxide layer width and beam convergence. The effects of plasmon scattering are included to first order in the lines marked B. It is assumed that a proportion of the electrons undergo an energy loss of 18 eV (a typical value of the range of plasmon losses in silicon) and that all these electrons are included in the aperture. The final profiles consist of an intensity addition of the remaining, purely elastically scattered electrons which continue to undergo elastic scattering (i.e. produce Fresnel contrast) after their inelastic scattering events.

phonon scattering. Based on the experimental fringe contrast derived from the thinnest parts of the specimen the oxide layer composition could be matched to that of the stoichiometric dioxide. While problems clearly remain with the quantification, the most important point to note is that the Fresnel method is still useful and quantifiably applicable for rather thin specimens. The accuracies attainable for unknown composition fluctuations must remain questionable because of the difficulties outlined above.

The final variable available in fitting Fresnel fringe profiles to simulations is the shape of the local scattering potential discontinuity which will differ from that of an abrupt square well if the composition of the oxide adjacent to the silicon varies gradually from SiO_2 through SiO_x to Si. It is demonstrated in fig. 5 that the detailed form of the Fresnel profile is sensitively dependent upon the shape of the potential well. Thus the thickness and shape of the oxide layer as determined by the Fresnel method can be compared with the measurements of the width of the amorphous layer

using high resolution methods. It was found for the early stages of oxidation when the oxide layer is less than 2 nm in thickness the width of the oxide layer derived from the Fresnel profiles is ~ 0.25 nm less than that derived from HREM images. However, for a 4 nm oxide layer the layer width derived from the Fresnel data is about 1 nm greater than that indicated by HREM imaging. These results have been interpreted as indicating that, as the oxide thickness is increased between 2 and 4 nm, the interface structure changes from {Si/amorphous SiO_x/SiO_2} to {Si/crystalline SiO_x/amorphous SiO_x/SiO_2}. The structure of the crystalline SiO_x has not been determined, in that we believe its projection is non-uniform for a typical foil thickness, but Ourmazd et al. [25] have described high resolution data in terms of there being a thin crystalline oxide layer from the onset of oxidation. The significance of the results we describe in terms of the oxidation mechanisms is that our data suggest this crystalline layer is not formed during the early stages of oxidation but only once the process is well established.
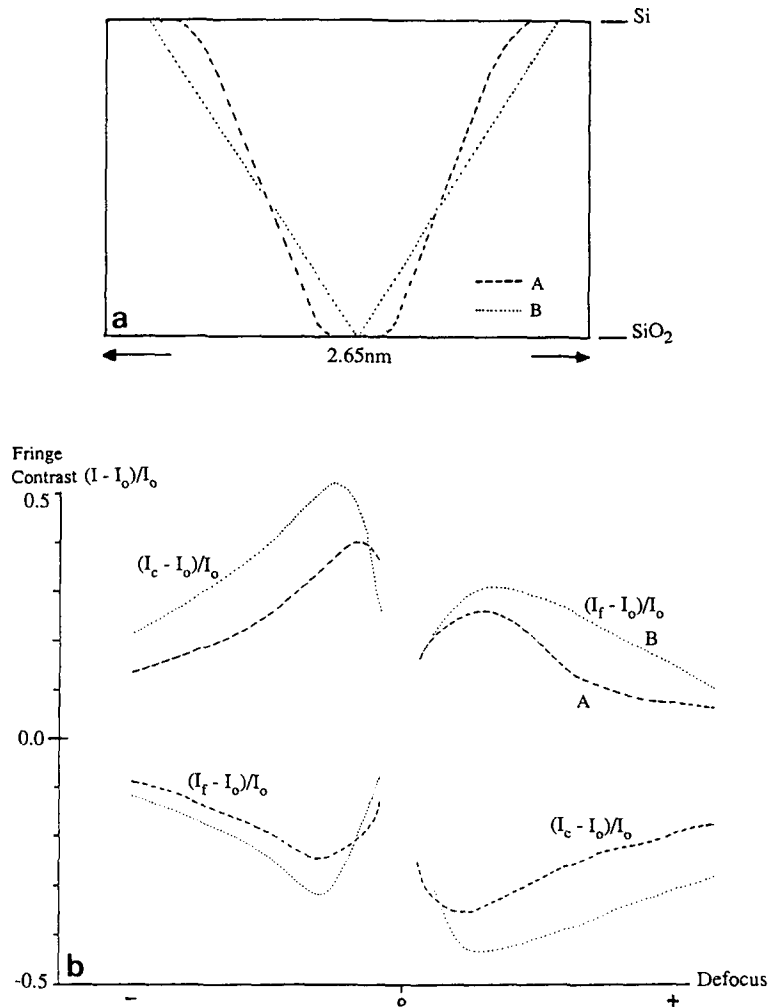
Fig. 5. In (a) two different composition profiles are shown, with B having a more gradual transition from Si to SiO_2, i.e. a thicker layer of nonstoichiometric SiO_x. It can be seen in (b) that these two models produce different fringe contrast/defocus graphs. The fringe spacing/defocus graphs (not shown) are very similar to each other. In the simulation the specimen thickness was 30 nm, the beam convergence was 0.55 mrad and the interfaces were assumed to be vertical. The defocus range is −1000 nm to +1000 nm.

3.2. Grain boundary segregation

We are currently applying the Fresnel approach to the characterisation of grain boundary segregation; an application of the method which, in principle, should provide a fruitful means of understanding the processes involved. Fresnel data for $\Sigma 3$ boundaries in copper obtained some years ago [26] could not be interpreted consistently with the more direct measurement of the boundary displacement obtained from lattice fringe shift mea-

surements [14] unless grain boundary segregation had also occurred. We are currently attempting to apply the Fresnel approach to the characterisation of boron segregation in both iron and Ni–Al. Our work on the Si/SiO_2 system also, of course, indicates that it should be possible to determine changes in the local concentration of a segregant, as would be expected to be caused by different thermal histories. In general, however, we are finding that there are two main difficulties in applying the Fresnel technique quantitatively to this type of
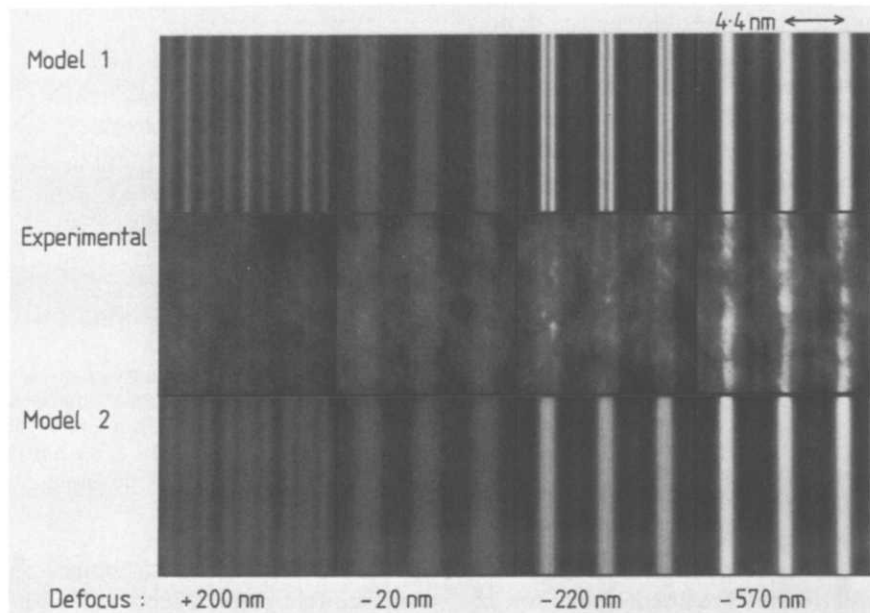
Fig. 6. Experimental and simulated images from a through focal series of bright field images of a 4.4 nm wavelength Cu/Ni–Pd multilayer. Model 1 contains one intermixed atomic layer on either side of the interfaces; in model 2 intermixing extends over two atomic layers on either side of the interfaces.

problem: firstly if the segregation causes, as it will, a change in the rigid body displacement at the boundary this cannot be determined independently of the composition change for a general high Σ grain boundary; and, secondly, it appears that differences in the inelastic scattering behaviour of an element such as boron by comparison with that of iron, as well as in the angular distribution of the elastic scattering, modify the Fresnel imaging behaviour in ways which it is difficult to simulate. Thus while we are seeing changes in the typical Fresnel scattering associated with grain boundaries when there is and is not local segregation we are currently unable to quantify our results.

3.3. Strained multilayers

For strained multilayers, as exemplified by the Cu/Ni–Pd system or semiconductor systems such as GaAs/InGaAs and Si/Si–Ge, the variation in lattice parameters from layer to layer is frequently the structural feature of greatest interest. However, before this can be determined it is imperative

that the composition profile is measured accurately since this will influence the interpretation of high resolution results. We have characterised Cu/Ni–Pd multilayer structures for a range of modulation wavelengths [17,27,28] and the first step in the quantitative procedure is to determine the degree of interdiffusion across the Cu/Ni–Pd interfaces. This can be done by comparison of the Fresnel profile in a bright field through-focal series with simulated images. Examples of the type of images and simulations which have been matched are shown in fig. 6. The sensitivity of the tech-
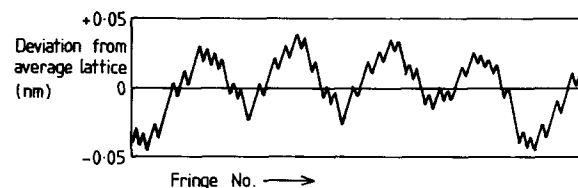

Fig. 7. Deviations from the average lattice of the measured positions of fringes in a non-axial lattice image of a 4.4 nm Cu/Ni–Pd multilayer. The periodic variation of the fringe spacings can be clearly seen and this corresponds to a maximum variation in the fringe spacings of 9%.

nique to small amounts of interdiffusion is demonstrated by comparing the fine detail of the middle row of experimental images with the best-fitting simulated images in the top row for which one atomic layer on either side of the interface has been allowed to intermix. If, instead, intermixing is allowed over two layers on each side of the interface, as was the case for the simulation shown in the bottom row of fig. 6, then the match with the experimental images is significantly degraded. The next stage in a characterisation of this sort of system is to measure the deviations of the individual lattice fringes from their averaged positions, thus in principle allowing a measurement of the strains present. An example of the approach is shown in fig. 7. For short wavelength multilayers, or systems such as Au/Ag with very little variation of lattice parameter, the shifts in fringe position are too small to be measured. Even for a highly strained Cu/Ni–Pd multilayer the small average lattice parameter $(d(002) = 0.18$ nm) means that it is essential to use non-axial high resolution imaging in order to obtain sufficient resolution to measure the *variation* in fringe positions [16]. This less conventional approach to lattice imaging is acceptable here, since it is spacing variations we are concerned with and not local atomic positions. The experimental images obtained for a 4.4 nm wavelength Cu/Ni–Pd multilayer were found to exhibit a variation in the lattice fringe spacing of up to 9%, depending on the objective defocus. However, simulated images calculated using the composition profile derived from the Fresnel technique indicated that a best fit with the variations in *fringe* spacing required only a 6% variation in *lattice* spacing.

In general considerable care has to be taken in the interpretation of both high resolution and low resolution images of strained layers, the intrinsic problems being exacerbated by stress relaxation at the surface of the foil [29]. This has two main effects: firstly, a thin TEM specimen is not truly representative of the bulk material, and secondly the bent lattice planes close to the foil surfaces produce strong contrast effects in the TEM images. For example, overlapping layers will often appear to be vertical layers of a different spacing [30]. The problems are perhaps best exemplified by
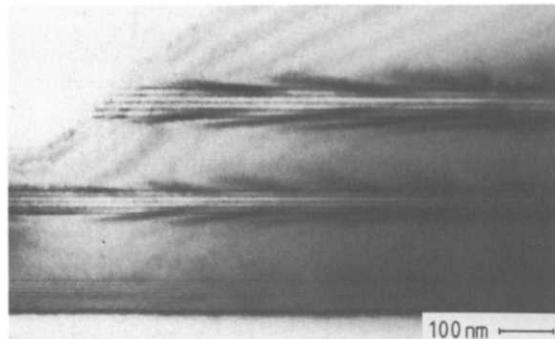

Fig. 8. Bright field image of three groups of five InGaAs layers in a GaAs matrix. The "fishbone" contrast seen extending into the GaAs is the result of the relaxation of the coherency strains in the groups of InGaAs layers at the surfaces of the cross-sectional specimen.

GaAs/InGaAs heterostructures: the extent of the surface relaxation which can arise in this type of strained system is demonstrated by the fishbone contrast that extends into the GaAs from the InGaAs in fig. 8.

3.4. GaAs / AlGaAs heterostructures

For semiconductor multilayers the features of most interest are: (1) the form of the composition modulation, i.e. the layer thickness, composition and diffuseness, (2) the misorientation of the growth direction from the cube normal (its vicinality), and (3) the form of any interface steps or dislocations present.

The form of the composition modulation is best determined by quantitative dark field methods to determine the Al content of a layer to a resolution of about 0.5 nm. It should, however, be noted that the technique does not have universal application for III–V systems, in that the InGaAs ternary alloy exhibits anomalous 002 intensities, and current results indicate that inelastic scattering is, if not uniquely responsible, at least contributing to the effect [9]. If higher spatial resolution is required it has been demonstrated that it can be achieved, at least for the binary AlAs/GaAs interface, using the Fresnel technique [31]. For MBE grown AlAs/GaAs layers the composition is generally considered to change over approximately one monolayer. However, quantitative analysis of
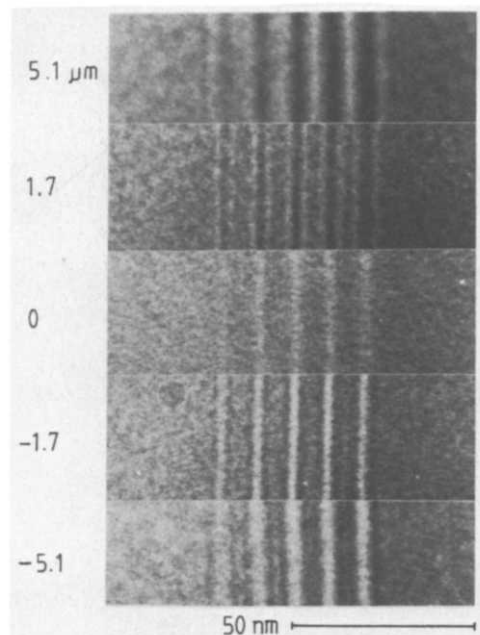
5.1 μm

1.7

0

-1.7

-5.1

50 nm

Fig. 9. Part of a Fresnel defocus series from a heterostructure consisting of five unequal layers of AlAs in GaAs. The defocus is shown at the left.

a series of images of a structure of five unequal AlGaAs layers in GaAs (fig. 9) has shown that the layers can, in fact, be diffuse over several monolayers [31].

It should, however, be noted that the determination of the layer composition from the Fresnel data is complicated (as was pointed out above) by the need to take account of the differing "absorption" of the materials present, and this proved to be difficult even for GaAs and AlAs in the work described above. For layered systems with very different scattering behaviours such as are necessarily present in X-ray mirrors (containing, for example, W and Si) the problem is considerably greater [12]. Various means of dealing with this problem are currently being investigated. We have tried including additional noise with a suitable frequency distribution in the initial potential model when doing non-atomistic simulations which otherwise do not lead to scattering outside the objective aperture, but a more fruitful approach appears to be to fit an imaginary component of the potential to the intensity differences

seen at zero defocus. Even then for W/Si multilayers difficulties remain as a result of the strong phase changes caused by the different layers.

The vicinality of an artificially formed multilayer is relatively straightforward to determine from a combination of 002 dark field and high resolution images, and from this an average step density can be inferred if the step height is assumed. However, it is much more difficult to image actual steps at, for example, a GaAs/Al GaAs interface. This is because the contrast exhibited by GaAs and AlAs in high resolution images is similar at thicknesses below those at which inelastic scattering again becomes important. In addition, it is expected that the steps will be aligned along $\langle 110 \rangle$ directions so that they will only be visible in HREM images when the beam is along the same $\langle 110 \rangle$ direction, and at this orientation the compositional contrast is reduced still further because of dynamical scattering to 002 from the $\{111\}$ reflections.

In an attempt to determine the importance or otherwise of inelastic scattering in high resolution imaging of local defects and steps an analysis has been made of images which would be formed when using a centre stop aperture to prevent the 000 beam from contributing to the image. Such a technique should improve considerably the visibility of the layers, as is demonstrated in fig. 10a for a GaAs/AlGaAs multilayer tilted a few degrees from [001]. Unfortunately, experimental centre stop images (fig. 11a) not only show no improvement in layer contrast but have a fringe periodicity of 0.28 nm, twice that which would be expected from the simulated images. The explanation for this is that, in order to obtain sufficient intensity in the centre stop image, the convergence is usually increased until the stop only just masks the 000 beam. Under these conditions electrons which are inelastically scattered through small angles can pass around the centre stop and contribute to the image, not only directly and incoherently to the background (as is usually assumed), but also through their further elastic scattering contribution to the atomic resolution detail. Based on the estimate (which can be justified both experimentally and theoretically) that 50% of the inelasticity scattered electrons pass around the
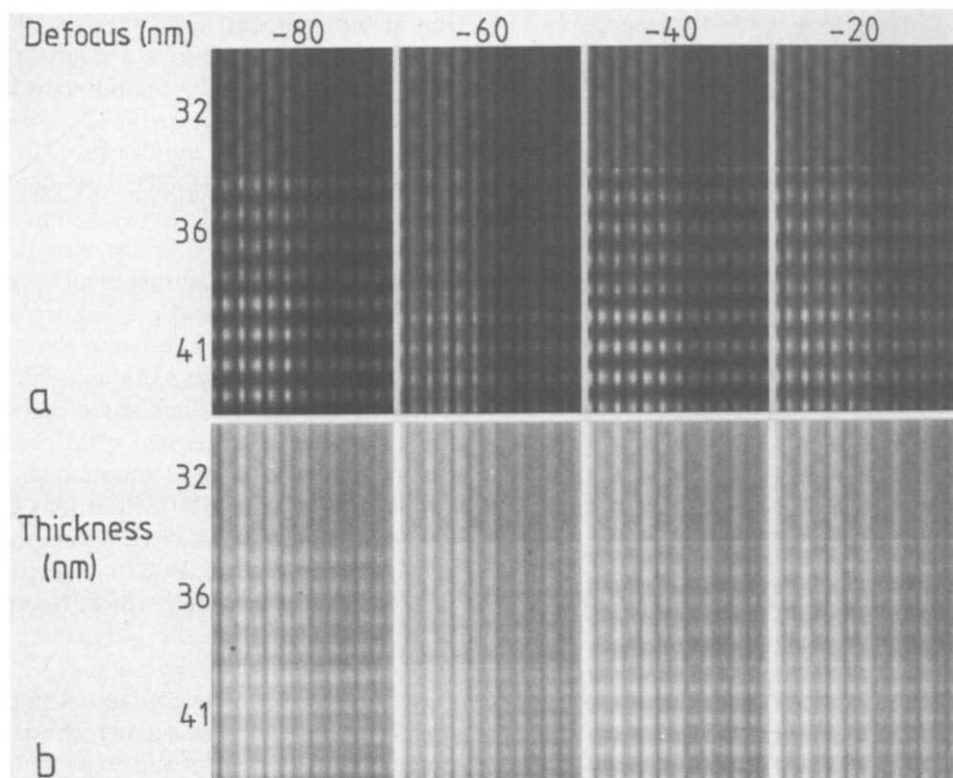
Fig. 10. Simulated images for an $Al_{0.3}Ga_{0.7}As/GaAs$ interface (GaAs on the right) imaged with the beam tilted by 4.3° from [100] about the interface normal, and the 000 beam excluded by a 0.6 nm radius centre stop aperture. In (a) only the effects of elastically scattered electrons are considered whilst in (b) the contribution from electrons scattered inelastically around the centre stop is also included.

centre stop for the conditions normally used, a simulation of the form of the image to be expected is shown in fig. 10b. The layer contrast is now much reduced and the larger 0.28 nm fringe spacing is beginning to dominate in the manner which is observed experimentally. Centre stop images have also been taken with lower convergences, as shown in fig. 11b, and the inferences drawn above are confirmed by the fact that the 0.14 nm fringes are now visible. However, reducing the convergence does not prevent inelastic scattering from occurring, so it would appear that accurate characterisation of interfacial steps using centre stop HREM will have to wait until energy-filtering high resolution microscopes become available. In the meantime, other still more indirect approaches will have to be applied (such as reflection imaging

(e.g., ref. [5])) in attempts to characterise local features of interfaces.

An important inference to be drawn from the above work is, however, that inelastic scattering contributions can make the normal interpretation of at least local composition variations in high resolution images non-viable, as has been predicted by Stobbs and Saxton [21]. In this context it is thus interesting that the [100] and [010] images of $YBa_2Cu_3O_{7-\delta}$ are substantially altered when the effects of inelastic scattering are included [32,33]. While the currently popular problem in HREM is the assessment of the accuracy to which O–Cu–O ordering can be evaluated by the comparison of such images, and the further understanding of inelastic contributions is clearly required for this, it will only be when this latter effect has been
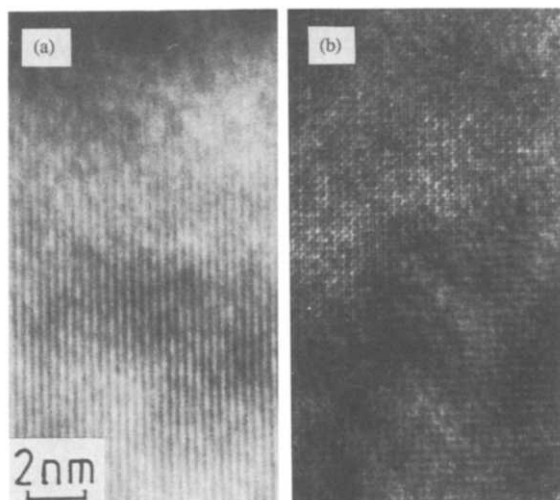
Fig. 11. Experimental centre stop images of GaAs/AlGaAs multilayers taken with (a) a relatively high convergence and (b) a much lower convergence. In (b) the contributions from inelastic scattering are much reduced so that the 0.14 nm fringes are now visible.

understood that the more important characterisation of the twin and grain boundaries in the material can be tackled.

4. Conclusion

It is not accidental that, just as artificially layered materials are being developed with properties which can only be optimised through a thorough understanding of the interfaces which these structures contain, so too are we seeing the development of new TEM techniques allowing characterisation at the required level. Many of the new TEM methods described here have proved to be successful for the specific purposes for which they were developed, but further refinement will be required before they can be applied more generally.

References

[1] D.G.H. Cockayne, I.L.F. Ray and M.J. Whelan, Phil. Mag. 20 (1969) 1265.
[2] H. Kakibayashi and F. Nagata, Japan. J. Appl. Phys. 24 (1985) L905.
[3] H. Kakibayashi and F. Nagata, Japan. J. Appl. Phys. 25 (1985) 1644.
[4] D.J. Eaglesham, C. Hetherington and C.J. Humphries, Mater. Res. Soc. Symp. Proc. 77 (1987) 473.
[5] C.B. Boothroyd, E.G. Britton, F.M. Ross, C.S. Baxter, K.B. Alexander and W.M. Stobbs, in: Microscopy of Semiconducting Materials, 1987, Inst. Phys. Conf. Ser. 87, Ed. A.G. Cullis (Inst. Phys., London–Bristol, 1987) p. 15.
[6] K. Sato and W.M. Stobbs, in: Microscopy of Semiconducting Materials 1987, Inst. Phys. Conf. Ser. 87, Ed. A.G. Cullis (Inst. Phys., London–Bristol, 1987) p. 253.
[7] P.M. Petroff, J. Vacuum Sci. Technol. 17 (1980) 1128.
[8] E.G. Britton, PhD Thesis, University of Cambridge (1987).
[9] C.S. Baxter, W.M. Stobbs, K.J. Monserrat and J.M. Tothill, in: Analytical Electron Microscopy, Ed. G.W. Lorimer (Inst. Metals, London, 1988) p. 209.
[10] J.N. Ness, W.M. Stobbs and T.F. Page, Phil. Mag. A54 (1986) 679.
[11] F.M. Ross and W.M. Stobbs, Surface Interface Anal. 12 (1988) 35.
[12] W.C. Shih, private communication.
[13] K.M. Knowles, F.M. Ross and W.M. Stobbs, in: Analytical Electron Microscopy, Ed. G.W. Lorimer (Inst. Metals, London, 1988) p. 55.
[14] G.J. Wood, W.M. Stobbs and D.J. Smith, Phil. Mag. A50 (1984) 375.
[15] W.M. Stobbs, G.J. Wood and D.J. Smith, Ultramicroscopy 14 (1985) 145.
[16] D.J. Hall, P.G. Self and W.M. Stobbs, J. Microscopy 130 (1983) 215.
[17] C.S. Baxter and W.M. Stobbs, Nature 322 (1986) 814.
[18] J.Y. Laval, C. Delamarre, A. Dubon, G. Schiffmacher, G. de Sagy and B. Guenais, in: Electron Microscopy and Analysis 1985, Inst. Phys. Conf. Ser. 78, Ed. G.J. Tatlock (Inst. Phys., London–Bristol, 1986) p. 359.
[19] Y. Suzuki and H. Okamoto, J. Appl. Phys. 58 (1985) 3456.
[20] C.B. Boothroyd and W.M. Stobbs, Ultramicroscopy 26 (1988) 361.
[21] W.M. Stobbs and W.O. Saxton, J. Microscopy 151 (1988) 171.
[22] P.E. Donovan and W.M. Stobbs, J. Microscopy 130 (1983) 361.
[23] P.E. Donovan and W.M. Stobbs, Ultramicroscopy 23 (1987) 119.

[24] F.M. Ross and W.M. Stobbs, in: Mater. Res. Soc. Symp. Proc. 105, Eds. G. Lucovsky and S.T. Pantelides (Mater. Res. Soc., Pittsburgh, PA, 1988).

[25] A. Ourmazd, D.W. Taylor, J. Rentschler and J. Bevk, Phys. Rev. Letters 59 (1987) 213.

[26] C.B. Boothroyd, A.P. Crawley and W.M. Stobbs, Phil. Mag. A54 (1986) 663.

[27] C.S. Baxter, in: Proc. 11th Intern. Congr. on Electron Microscopy, Kyoto, 1986, Eds. T. Imura, S. Maruse and T. Suzuki (Japan. Soc. Electron Microscopy, Tokyo, 1986) p. 1479.

[28] C.S. Baxter and W.M. Stobbs, in: Electron Microscopy and Analysis 1985, Inst. Phys. Conf. Ser. 78, Ed. G.J. Tatlock (Inst. Phys., London–Bristol, 1986) p. 387.

[29] M.J. Treacy, J.M. Gibson and A. Howie, Phil. Mag. A51 (1985) 389.

[30] C.S. Baxter and W.M. Stobbs, Appl. Phys. Letters 48 (1986) 1202.

[31] F.M. Ross, E.G. Britton and W.M. Stobbs, in: Analytical Electron Microscopy, Ed. G.W. Lorimer (Inst. Metals, London, 1988) p. 205.

[32] M.J. Hÿtch and W.M. Stobbs, in: Proc. 46th Annual EMSA Meeting, Milwaukee, WI, 1988, Ed. G.W. Bailey (San Francisco Press, San Francisco, 1988) p. 958.

[33] M.J. Hÿtch and W.M. Stobbs, in: Proc. EUREM 88, Vol. 2, Inst. Phys. Conf. Ser. 93, Eds. P.J. Goodhew and H.G. Dickinson (Inst. Phys., London–Bristol, 1988) p. 347.